Nitrogenase Reactivity: Effects of Component Ratio on Electron Flow and Distribution during Nitrogen Fixation†

Scot Wherland,‡ Barbara K. Burgess,* Edward I. Stiefel, and William E. Newton

ABSTRACT: The nature of the interaction between the two component proteins of nitrogenase and the mechanisms of H_2 evolution, N_2 fixation, and H_2 inhibition of N_2 reduction are probed by variations in the *Azotobacter vinelandii* Fe protein/MoFe protein (*Av*2/*Av*1) ratio (from 0.1 to 140) and their effect on total electron flow and the partitioning of that flow to products. The following conditions are used: (1) 100% Ar; (2) 100% D_2; (3) 50% D_2/50% Ar; (4) 100% N_2; (5) 40% N_2/60% Ar; (6) 50% D_2/40% N_2/10% Ar; and (7) 30 mM hydrazine under argon. For these sets of conditions, plots of activity vs. the *Av*2/*Av*1 ratio are similar in form, peaking at a ratio between 3 and 5. HD formation accounts for 6% and 9% of the total electron flow under 50% D_2/50% Ar and 100% D_2, respectively, with the percentage being independent of the *Av*2/*Av*1 ratio. Under 50% D_2/40% N_2/10% Ar, HD formation increases to 25% of the total electron flow and is dependent upon the *Av*2/*Av*1 ratio. Ammonia formation increases from 0% to 40% of the total electron flow under 40% N_2 as the *Av*2/*Av*1 ratio increases from 0 to 5. At *Av*2/*Av*1 ratios of 5–140, NH_3 formation further increases to 60% of the total electron flow, which is the maximum observed under 100% N_2. All experiments involving N_2 show a slight decrease in total electron flow over those without N_2. Generally, the lower *Av*2/*Av*1 ratios favor H_2 evolution and HD formation over NH_3 production. This effect has been termed *Av*1 inhibition of *Av*2 activity but is more appropriately visualized in terms of changing electron allocation. The observations made provide a basis for testing mechanisms for nitrogenase-catalyzed N_2 reduction, HD formation, and H_2 evolution. A mechanism is presented for which good agreement is found between the calculated and observed plots of activity vs. component ratio and for the data normalized to *Av*1. This mechanism, however, fails to predict the decrease in *Av*2 activity for NH_3 production and the tendency to favor H_2 evolution over NH_3 formation, both of which occur at low *Av*2/*Av*1 ratios.

Nitrogen fixation and all other reductions catalyzed by the nitrogenase system require two easily separated component proteins, called the molybdenum–iron protein (MoFe protein) and the iron protein (Fe protein). The physical properties of these two proteins have been recently reviewed (Orme-Johnson et al., 1977; Mortenson & Thorneley, 1979), and great similarity among proteins from different bacterial sources is evident (Emerich & Burris, 1976a,b). In addition to these two proteins, a source of reducing equivalents, MgATP,[1] and protons are required for all substrate reductions (Bulen & LeComte, 1966). The MoFe protein is believed to contain the site of substrate reduction (Shah et al., 1973; Smith, 1977; Hageman & Burris, 1978), while the Fe protein is generally accepted as the specific one-electron donor for the MoFe protein (Hageman & Burris, 1978a,b; Ljones & Burris, 1978). Two aspects of the nitrogen-fixation reaction, which are especially intriguing and which we will address herein, are the nature of the interaction between the two proteins and the mechanism of the energetically wasteful hydrogen evolution and hydrogen inhibition reactions of nitrogen fixation (Winter & Burris, 1976; Orme-Johnson et al., 1977).

One extensively pursued possibility for the interaction of the MoFe and Fe proteins is that the two proteins form a tight complex of defined stoichiometry which does not dissociate during turnover (Eady, 1973; Thorneley et al., 1975). In fact, Bulen & LeComte (1966) successfully isolated a particulate complex directly from *Azotobacter vinelandii* (*Av*) cells, which contains an Fe/MoFe protein ratio close to 1 and at least one additional protein (Haaker & Veeger, 1977). Dilution studies on this complex (Silverstein & Bulen, 1970), as well as on complexes formed by recombining purified components from *Klebsiella pneumoniae* (*Kp*) and *Azotobacter chroococcum* (*Ac*) (Thorneley et al., 1975), show a greater loss of activity than would be predicted merely from dilution. Such data have been interpreted in terms of a one-to-one complex with protein–protein binding constants on the order of 10^7 M^{-1}. However, these data have been fitted to other models equally well (Orme-Johnson et al., 1977). Also, a two-to-one (albeit inactive) complex is formed between *Clostridium pasteurianum* (*Cp*) Fe protein and *Av* MoFe protein (Emerich & Burris, 1976a,b).

An alternative treatment considers the Fe protein as a cosubstrate for the MoFe protein (Bergerson & Turner, 1973) with the two proteins dissociating during turnover. Hageman & Burris (1978a,b), working primarily at very low Fe/MoFe protein ratios, found an apparent lag in H_2 evolution but not in ATP hydrolysis, which is consistent with the Fe protein acting as a specific reductant for the MoFe protein and dissociating from it after every electron transfer. Their results, which suggest transient one-to-one and two-to-one complexes with lifetimes no longer than one catalytic cycle, rely partially on their dithionite oxidation kinetics showing saturation at high (5–15 mM) dithionite concentrations. This observation is in direct contrast to other studies (Watt & Burns, 1977; Watt, 1980). However, additional support for the transient complex interpretation comes from electron paramagnetic resonance

† Contribution No. 732 from the Charles F. Kettering Research Laboratory, Yellow Springs, Ohio 45387. *Received July 29, 1980; revised manuscript received April 2, 1981.* This study was supported in part by Project No. 7900359 from SEA/CGO of the U.S. Department of Agriculture. S.W. was supported by a National Science Foundation National Needs Postdoctoral Fellowship.

‡ Present address: Department of Chemistry, Washington State University, Pullman, WA 99163.

[1] Abbreviations used: ATP, adenosine 5′-triphosphate; EPR, electron paramagnetic resonsance; Tes, *N*-tris(hydroxymethyl)methyl-2-aminoethanesulfonic acid.

0006-2960/81/0420-5132$01.25/0

(EPR) spectral analyses under pre-steady-state conditions (Hageman & Burris, 1979).

Maximum specific activities of the isolated component proteins are attained at Fe/MoFe protein ratios which vary with the component protein assayed, the substrate reduced, and the bacterial source (Eady et al., 1972; Shah et al., 1972; Mortenson et al., 1976; Hageman & Burris, 1978b). Under the usual assay conditions, the specific activity of the Fe protein does not show simple saturation behavior but peaks at a specific Fe/MoFe protein ratio. This phenomenon has been attributed to inhibition by excess MoFe protein (Ljones & Burris, 1972). Titrations of the MoFe protein with the Fe protein behave more typically. The MoFe protein activity plateaus or, at least, increases much less rapidly with Fe protein concentration at Fe/MoFe protein ratios above ~10 (Eady et al., 1972; Mortenson et al., 1976; Hageman & Burris, 1978b), depending on the concentration of the protein, salt, ATP, and reductant, as well as temperature and sometimes the substrate being considered. Difficulties in defining the Fe/MoFe protein ratios giving these maximal individual activities arise because of the varying purity of the proteins used, especially the Fe protein. The Fe/MoFe protein ratio which gives optimal nitrogenase turnover can also be determined by such titrations (Vandercasteele & Burris, 1970; Mortenson et al., 1976) and for *Cp* is found to be 2. Thus, although complexes between the two components exist, their stoichiometry and especially their lifetime remain an active and controversial topic.

The second aspect for consideration is the energetically wasteful H_2 evolution and H_2 (D_2) inhibition reactions of N_2 fixation. In the absence of other reducible substrate, all reductant consumed by nitrogenase is used in ATP-dependent H_2 evolution (Bulen et al., 1965). When N_2 is added, some electron flow continues to support H_2 evolution (Hadfield & Bulen, 1969; Rivera-Ortiz & Burris, 1975). Analyses of electron distribution have produced contradictory predictions that either N_2 reduction can completely eliminate H_2 evolution (Davis et al., 1975) or the limiting stoichiometry is one H_2 evolved per N_2 reduced. The situation is further complicated by H_2 being a specific inhibitor of N_2 reduction (Wilson & Umbreit, 1937; Hwang et al., 1973) and because, under D_2 with H_2O or H_2 with D_2O, nitrogenase catalyzes the formation of HD [Hoch et al., 1960; see also Burgess et al. (1981)]. The present study attempts to define the effect of a wide range of Fe/MoFe protein ratios on total electron flow and on the partitioning of electron flow to products, particularly under varying atmospheres of N_2 and H_2 (D_2). We focus on the multifaceted H_2 reactions of nitrogenase because of their importance for our understanding of the mechanism of N_2 reduction.

Materials and Methods

Nitrogenase Assay. *A. vinelandii* MoFe and Fe protein, designated *Av*1 and *Av*2, respectively, were purified and analyzed as described elsewhere (Burgess et al., 1980). All assays were performed at 30 °C in 9.5-mL calibrated vials, fitted with butyl rubber serum stoppers and metal caps, containing the appropriate gas mixture. The 1.0-mL reaction mixture contained 38 mM Tes–KOH (pH 7.4), 2.5 mM ATP, 5.0 mM $MgCl_2$, 30 mM creatine phosphate, 20 mM neutralized $Na_2S_2O_4$, 0.125 mg of creatine phosphokinase, and enough NaCl to give a final concentration of 20 mM, thus eliminating the variable salt levels produced by adding different amounts of *Av*2 and *Av*1. A constant concentration of MgATP was maintained by the ATP-generating system, and excess sodium dithionite was used to minimize MoFe protein inhibition of the Fe protein (Hageman & Burris, 1978b). The vessel containing the reaction mixture was degassed and filled with the appropriate gas mixture by using a published procedure (Corbin, 1978), $Na_2S_2O_4$ was added, followed by *Av*2, and the reaction was started by adding *Av*1 to give the appropriate molar ratio of the two components. A total of 1 mg of protein per 1-mL reaction was used to avoid complications introduced by large protein concentrations.

For *Av*2/*Av*1 ratios <0.5 or >20, 20-min reaction times were used; otherwise, reactions were run for 10 min. Reactions were terminated with 0.25 mL of 2.5 M H_2SO_4. Separate experiments under 100% Ar, 50% D_2/40% N_2/10% Ar, and 50% D_2/50% Ar showed that product formation was linear with time. All data are reported as nanomoles of product formed per minute per milligram of *total protein* and, therefore, do not correspond to the specific activity of either component protein.

Product Analysis. In all experiments, *all products were measured on the same reaction vial.* All data points represent means of, typically, triplicate determinations (see paragraph at end of paper regarding supplementary material). If D_2 was not present, 200-μL gas samples, in a pressure-lock syringe (Precision Sampling) at bottle pressure, were analyzed for H_2 by gas chromatography using a thermal conductivity detector and a molecular sieve 5A column. The gas chromatograph was calibrated by using standards containing 1.0% H_2, balance Ar (Applied Science Laboratories, Inc., State College, PA). If D_2 was present, gas samples were expanded to a fixed volume in a Finnigan mass spectrometer, and the spectrum was recorded at a preset time after expansion. The sensitivity at each mass was measured by commercially standardized gas mixtures (Matheson), except for HD which was formed from $LiAlH_4$ and D_2O in an evacuated vessel. *Caution is advised when performing this reaction.* Standards and backgrounds were analyzed at regular intervals during each day of measurement. After gas samples were analyzed, 1 mL of saturated K_2CO_3 was added to the acid-quenched reaction mixture, and the samples were microdiffused with shaking overnight (Burris, 1972). The rods were washed in 3.75 mL of a 0.14 M phenol solution, and then 0.1 mL of a freshly prepared 0.25 M $Na_2Fe(CN)_5NO$ solution was added followed immediately by 1.0 mL of a freshly prepared hypochlorite solution (100 mL of 0.75 M NaOH plus 2 mL of bleach). After 3 h, the absorbance at 625 nm was measured (Chaykin, 1969). A standard curve was run in duplicate with each experiment. All standard and control bottles were microdiffused.

Data Analysis. Controls containing the complete assay sysem with either 1 mg of *Av*2 or 1 mg of *Av*1 were run in triplicate while additional controls containing the gas mixture alone were run in sextuplicate. All gas mixtures containing D_2 also contained some H_2 and HD. The average values for this nonenzymatically produced H_2 and HD were calculated for the controls and subtracted from the raw data prior to further analysis. Some NH_3 was detected in all control vials with protein present, including controls containing reaction mixture without *Av*2 or *Av*1. The average of six vials containing 1 mg of *Av*2 alone or 1 mg of *Av*1 alone was subtracted as background from the final NH_3 data. For NH_3 formation with hydrazine present, additional controls were run in triplicate including the appropriate level of hydrazine and were also subtracted as background. Trivial zero-yield data, e.g., HD formed in the absence of D_2, were excluded.

Calculations. All data analyses were performed on an IBM 5100 desk-top computer using programs in the Basic language. The total number of nanomoles of H_2 in any vial was calcu-

lated, after subtracting the background H_2, by using the calibrated volume (minus 1.25 mL of liquid) without correcting for gas solubility and then converted to nanomoles per minute per milligram of protein. Mass spectrometric data were analyzed similarly to the gas chromatographic data, except that now three species (H_2, HD, and D_2) were being measured. For experiments under 50% D_2, increased precision was obtained by normalizing to the constant D_2 signal. For ammonia analysis, the standard curve was fitted to a parabola, and the equation for the parabola was used to convert absorbance to an absolute amount of ammonia for each vial.

Fitting of the acquired data to various mechanisms used the nonlinear least-squares program GRADLS (Bevington, 1969) (the computer program is available on request from S. Wherland at Washington State University, Pullman, WA). The equations for the rate of formation of each product were derived for each proposed mechanism by the methods of King & Altmann (1956), which led to an expression in terms of the rate constants, total *Av*2, *Av*1 (treated as the enzyme), and free *Av*2. A polynomial in powers of the concentration of uncomplexed *Av*2 concentration was derived from the expressions for the concentrations of each of the enzyme forms. This equation was solved numerically by Newton's method for the root closest to and less than the total *Av*2 concentration. The variables were the individual rate constants in each mechanism, which were varied under the control of the GRADLS program. Various initial guesses were used and various numbers of parameters were held constant during some iterations. For the χ^2 calculation, weighting factors were taken as the square of the reciprocal of the standard deviation associated with each point or 10%, whichever was greater. Reduced χ^2 is equal to χ^2/(number of observations − number of parameters).

Gases. All gases were of the highest purity available and analyzed by Matheson.

Chemicals. All chemicals were of the highest grade available from the Sigma Chemical Co., except creatine phosphate, which was synthesized according to published methods (Anatol, 1961), and bleach, which was purchased locally.

Results

The experiments to determine the dependence of total electron flow and its distribution on the *Av*2/*Av*1 ratio use the following conditions: (1) 100% Ar; (2) 100% D_2; (3) 50% D_2/50% Ar; (4) 100% N_2; (5) 60% Ar/40% N_2; (6) 50% D_2/40% N_2/10% Ar; and (7) 100% Ar with 30 mM hydrazine in solution. For each experiment, 15–18 ratios of *Av*2/*Av*1, in the range 0.1–140, are studied. The results for all experiments in terms of the *Av*2/*Av*1 ratio, the mean number of nanomoles per minute per milligram of total protein of each product assayed, the standard deviation of the mean, and the number of replicates appear in supplementary material (Tables I–VII). The number of replicates is typically three.

The data are presented graphically in several ways. The first seven figures are numbered to correspond to the experimental conditions defined above. The *Av*2/*Av*1 ratio axis is identical in all figures with a scale change at 20. The most straightforward plot of the data is as yield vs. the *Av*2/*Av*1 ratio (part a of Figures 1–7). The data are also presented as titration curves after normalizing the yields to either 1 mg of *Av*1 (Figure 1b) or 1 mg of *Av*2 (Figures 1c and 6c). The trend in electron partitioning to products is most obvious in part b of Figures 3, 4, and 6, where percentage and total electron flow are calculated assuming (vide infra) three electrons per ammonia produced from N_2, two electrons per

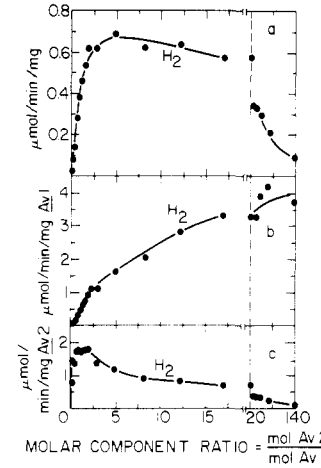

FIGURE 1: H_2 evolution by nitrogenase under an atmosphere of 100% Ar. Plots of (a) micromoles of H_2 formed per minute per milligram of total protein vs. component ratio, (b) micromoles of H_2 formed per minute per milligram of *Av*1 vs. ratio, and (c) micromoles of H_2 formed per minute per milligram of *Av*2 vs. ratio. ● represents H_2 evolved. *For all figures*, the molar component ratio is calculated on the basis of molecular weight values of 230 000 and 64 000 for *Av*1 and *Av*2, respectively. Assays and calculations were performed as described under Materials and Methods. Points represent means of typically triplicate determinations (see supplementary material). Lines drawn are visual fits through the data points. All products were measured on the same reaction vial. For all figures except Figure 6c, there is a scale change at a ratio of 20 with the last point before the break repeated.

H_2 evolved, one electron per HD formed (Bulen, 1976; Newton et al., 1977), and one electron per ammonia produced from hydrazine.

Figure 1a is a plot of the nanomoles of H_2 evolved per minute per milligram of total protein vs. the *Av*2/*Av*1 ratio under 100% Ar, where only protons are available for ATP-dependent H_2 evolution. This activity profile shows a rapid increase at the low *Av*2/*Av*1 ratios, a broad peak around an *Av*2/*Av*1 ratio of 5, followed by a gradual decrease out to the highest ratios tested. The curve is required to pass through 0 at *Av*2/*Av*1 ratios of 0 and infinity because each component protein lacks activity without the other. Parts b and c of Figure 1 illustrate the same data normalized to *Av*1 and *Av*2, respectively. This treatment simulates titration curves for both proteins [see, e.g., Davis et al. (1975)]; however, here specific activities are plotted vs. the *Av*2/*Av*1 ratio. The specific activity of *Av*1 increases with increasing *Av*2 concentration, most rapidly at ratios below 10. The *Av*1 specific activity does not level off at even the highest ratios tested, where a maximum of 3900 nmol of H_2 evolved min^{-1} (mg of *Av*1)$^{-1}$ is obtained. The *Av*1 activities and the general shape of the activity curves are extremely similar for all experiments. Figure 1c shows a maximum activity for *Av*2 of 1800 nmol of H_2 evolved min^{-1} (mg of *Av*2)$^{-1}$ between *Av*2/*Av*1 ratios of 0.7 and 1.9. Above and below these ratios, activity is lower in agreement with previous findings [e.g., Ljones & Burris (1978)].

When D_2 is present, ATP-dependent N_2-*independent* HD formation (Burgess et al., 1981) accompanies ATP-dependent H_2 evolution. Figures 2 and 3a are plots of nanomoles of product per minute per milligram of total protein vs. the *Av*2/*Av*1 ratio, under 100% D_2 and 50% D_2/50% Ar, respectively, and show a general shape similar to that of Figure 1a for both products. Figure 3b shows that, under 50% D_2/50% Ar, the percentage of the total electron flow going to each product vs. the *Av*2/*Av*1 ratio is *invariant* over the range of component ratios tested. The formation of HD uses

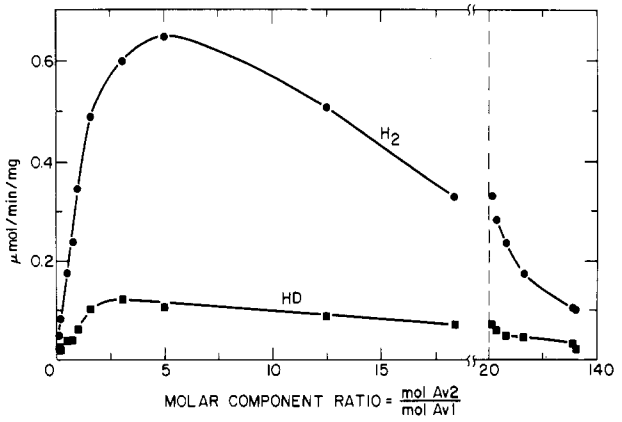

FIGURE 2: N_2-independent HD formation by nitrogenase under an atmosphere of 100% D_2. Plot of micromoles of product formed per minute per milligram of total protein vs. ratio. ● represents H_2 evolution and ■ HD formation. Details are given in the legend of Figure 1.

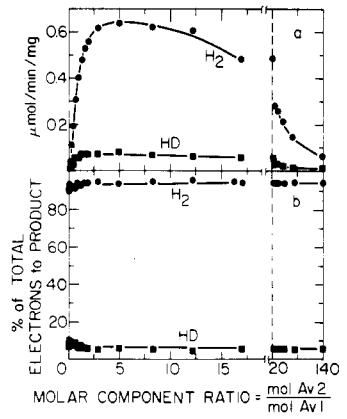

FIGURE 3: N_2-independent HD formation by nitrogenase under an atmosphere of 50% D_2/50% Ar. Plots of (a) micromoles of product formed per minute per milligram of total protein vs. ratio and (b) percentage of total electron flow going to each product vs. ratio. ● represents H_2 evolution and ■ HD formation. Details are given in the legend of Figure 1. Total electron flow and percentage calculations were performed as described in text.

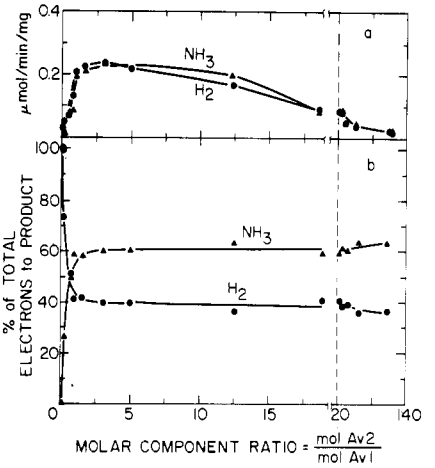

FIGURE 4: N_2 fixation by nitrogenase under an atmosphere of 100% N_2. Plots of (a) micromoles of product formed per minute per milligram of total protein vs. ratio and (b) percentage of total electron flow going to each product vs. ratio. ● represents for H_2 evolution and ▲ NH_3 formation. Details are given in the legends of Figures 1 and 3.

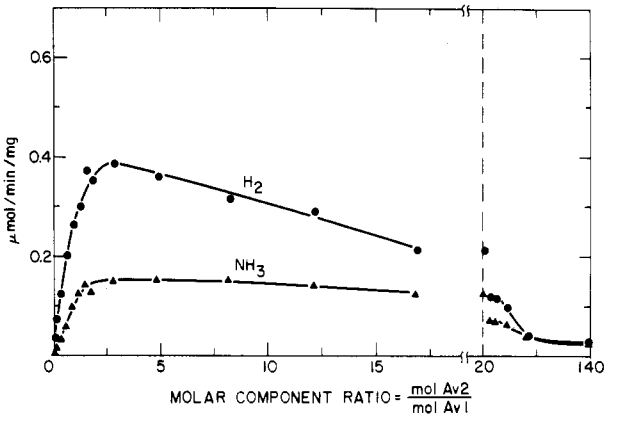

FIGURE 5: N_2 fixation by nitrogenase under an atmosphere of 40% N_2/60% Ar. Plot of micromoles of product formed per minute per milligram of total protein vs. ratio. ● represents H_2 evolution and ▲ NH_3 formation. Details are given in the legend of Figure 1.

an average of 9% of the electron flow under 100% D_2 and 6% under 50% D_2/50% Ar, i.e., doubling the D_2 partial pressure increases HD formation by only 50%. When normalized to *Av*2, these data show that the specific activity of *Av*2 levels off at ratios below 2 and does not decrease further at lower ratios for either product (not shown).

The nitrogen-fixation reaction of nitrogenase is illustrated in Figures 4a (100% N_2) and 5 (40% N_2/60% Ar) which show that ATP-dependent H_2 evolution accompanies N_2 reduction to ammonia with the same smooth variation with component ratio and broad activity maximum between the ratios 3 and 8. When the N_2 partial pressure is increased from 40% (Figure 5) to 100% (Figure 4a), the peak NH_3 activity shifts to a slightly lower ratio and increases by 50%. Figure 4b shows that, under 100% N_2, the percentage of electron flow used to form NH_3 increases sharply from 0% at a ratio of 0.1 to 60% at a ratio of 3 and remains roughly constant at the higher ratios. In contrast, under 40% N_2/60% Ar (not shown), 35–40% of the electron flow is giving NH_3 by a ratio of 5, but this continues to increase to 60% at the highest *Av*2/*Av*1 ratio. The data for our 100% N_2 and 40% N_2/60% Ar experiments, when normalized to *Av*2 (not shown), indicate *no* decrease in *Av*2 specific activity as measured by H_2 evolution at low ratios (high *Av*1). There is, however, a pronounced decrease in *Av*2 activity for NH_3 formation at ratios below 1.

Under an atmosphere of 50% D_2/40% N_2/10% Ar, three products, H_2, HD and NH_3, are measured. Figure 6a shows the great similarity in general shape and peak *Av*2/*Av*1 ratio among all three products and to those of the simpler systems. Figure 6b illustrates the partitioning of electron flow to the three products. The general trend in electron allocation to NH_3 and H_2 is similar to the 100% N_2 and 40% N_2/60% Ar experiments, where low *Av*2/*Av*1 ratios favor H_2 evolution over N_2 reduction. Total HD formation increases more rapidly than NH_3 formation and reaches its maximum share of electron flow of ~21% by a ratio of 1. When normalized to *Av*2 (Figure 6c), H_2 evolution shows no decrease at low ratios (high *Av*1), while there is a dramatic decrease in both NH_3 and HD formation as found for the 100% N_2 and 40% N_2/60% Ar experiments. Note that both total HD formation (Figure 6c) and N_2-dependent HD formation (Figure 6d) increase more steeply than does NH_3 formation to level off at a ratio of ~1.

Studies of the reduction of hydrazine, a possible intermediate in N_2 fixation, are reported in detail in the following paper (Burgess et al., 1981) and are shown in Figure 7. Under 100% Ar with 30 mM hydrazine present, both H_2 and NH_3 production show the same smooth variation with *Av*2/*Av*1 ratio as for other substrates. However, NH_3 formation peaks at a lower *Av*2/*Av*1 ratio (2) than for any other experiment while H_2 evolution still peaks around a ratio of 5. This difference

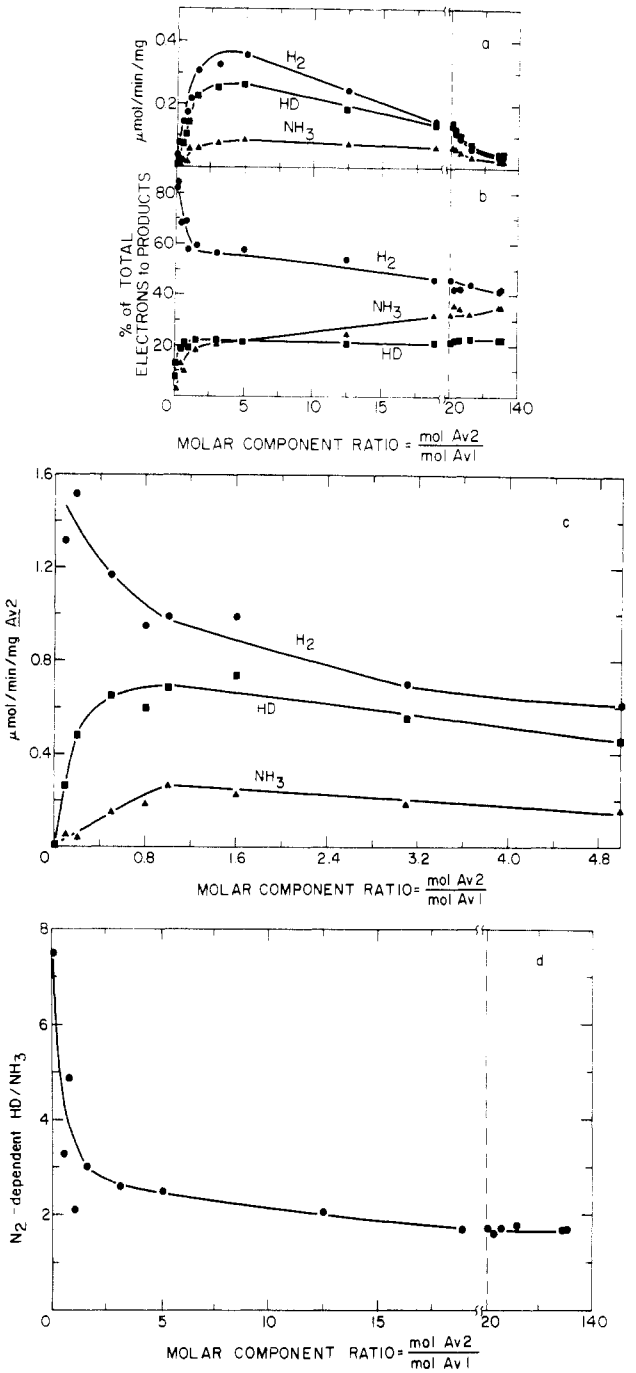

FIGURE 6: D_2-inhibited N_2 fixation by nitrogenase under an atmosphere of 50% D_2/40% N_2/10% Ar. Plots of (a) micromoles of product formed per minute per milligram of total protein vs. ratio, (b) percentage of total electron flow to products vs. ratio (details in the legends of Figures 1 and 3), and (c) micromoles of product formed per minute per milligram of *Av*2 vs. ratio (where ratio range is 0–4.8). For (a–c), ● represents H_2 evolution, ■ HD formation, and ▲ NH_3 formation. Plot of (d) micromoles of N_2-dependent HD per micromoles of NH_3 formed vs. ratio (●). N_2-dependent HD was calculated as described in text.

is better shown by the changes in the percentage of total electron flow going to NH_3 formation as a function of the *Av*2/*Av*1 ratio (not shown). It is level (at about 20–25%) at ratios below 8 but decreases to ~14% at the highest ratios. This observation is the only example for which high ratios decrease the electron allocation to a substrate other than protons.

Total electron flow through nitrogenase has been reported as largely independent of the substrate being reduced (Watt & Burns, 1977). However, when total electron flow under our

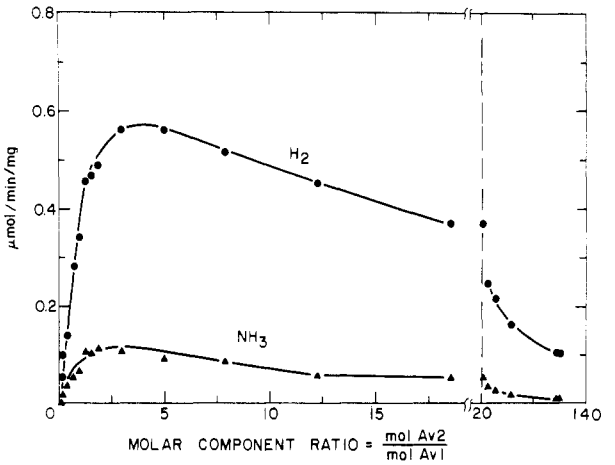

FIGURE 7: Hydrazine reduction by nitrogenase under an atmosphere of 100% Ar with 30 mM hydrazine present in solution. Plot of micromoles of product formed per minute per milligram of total protein vs. ratio. ● represents H_2 evolution and ▲ NH_3 formation. Details are given in the legend of Figure 1.

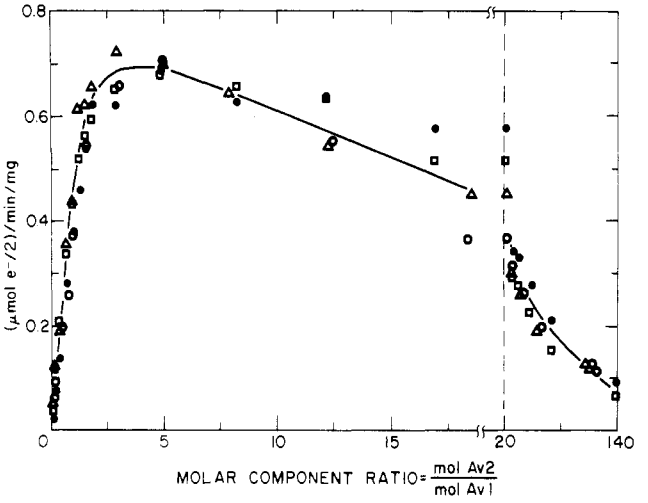

FIGURE 8: Total electron flow through nitrogenase in the absence of N_2. Plot of micromoles of total electron pairs of all products per minute per milligram of total protein vs. ratio for atmospheres of (●) 100% Ar, (○) 100% D_2, (□) 50% D_2/50% Ar, and (△) 100% Ar with 30 mM hydrazine. Details are given in the legends of Figures 1 and 3.

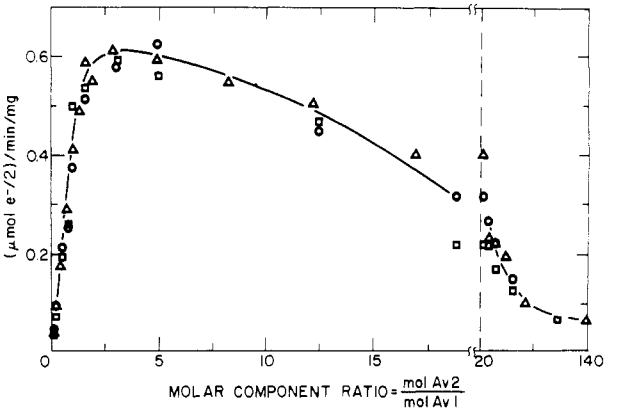

FIGURE 9: Total electron flow through nitrogenase in the presence of nitrogen. Plot of micromoles of total electron pairs to all products per minute per milligram of total protein vs. ratio for atmospheres of (□) 100% N_2, (△) 40% N_2/60% Ar, and (○) 50% D_2/40% N_2/10% Ar.

seven experimental conditions is compared, the data fall into two categories, those without N_2 (Figure 8; 100% Ar, 100% D_2, 50% D_2/50% Ar, and 100% Ar with 30 mM hydrazine) and those with N_2 (Figure 9; 100% N_2, 40% N_2/60% Ar, and

50% D_2/40% N_2/10% Ar). Although the general shape and peak ratios are the same for both Figures 8 and 9, the total electron flow drops from 0.70 ± 0.02 (without N_2) to 0.61 ± 0.02 (with N_2) nmol of electron pairs min^{-1} (mg of total protein)$^{-1}$, i.e., a 13% decrease.

Discussion

A general feature of all experiments is the shape of the *Av*2/*Av*1 ratio dependence of electron flow. All plots peak at *Av*2/*Av*1 ratios between 3 and 5. On the basis of a single complex with a high binding constant, the shape of the activity curves suggests that the most active complex would have a stoichiometry of three to five Fe proteins per MoFe protein. However, there is no evidence for either such high numbers of bound Fe proteins or the existence of a single long-lived complex (Hageman & Burris, 1978a,b; Orme-Johnson, et al., 1977). This shape would also be predicted by lower stoichiometry, lower binding constant complexes, which would peak in activity at *Av*2/*Av*1 ratios higher than the stoichiometric one because higher concentrations are required to saturate the binding sites. A mechanism in this general category is preferred and discussed below.

The maximum activity observed is similar in all experiments, which is consistent with electron flow being similar for all substrate reductions (Watt & Burns, 1977). However, a trend toward slightly lower electron flow (a 13% decrease) in the presence of N_2 is apparent when experiments 4–6 are compared with experiments 1–3 and 7. The same trend is observed in both polarographically monitored dithionite utilization and other data in the following paper (Burgess et al., 1981). A decrease in electron flow of up to 35% with increasing N_2 pressure was reported recently (Hageman & Burris, 1980), but this effect is much more dramatic than any that we have ever observed except for the formation of HD under N_2/D_2 mixtures. Hydrazine reduction, at 30 mM, behaves like the N_2-free reactions as far as electron flow is concerned. However, with an *Av*2/*Av*1 ratio of 5, hydrazine concentrations above 30 mM cause a decrease in total electron flow (Burgess et al., 1981).

The decrease in the specific activity of the Fe protein at ratios below 1 (excess MoFe protein) is a significant feature of nitrogenase kinetics. In the *Av*2/*Av*1 ratio range 0.1–1.0, 20 mM dithionite nearly eliminates this inhibition in the H_2 evolution assay (Hageman & Burris, 1978b). With 20 mM dithionite present, we see *Av*2 specific activity, for total electron flow, reach a maximum around an *Av*2/*Av*1 ratio of 2 and remain constant at lower ratios. The one exception is our 100% Ar experiment (Figure 1c) where a slight decrease in *Av*2 specific activity is evident at *Av*2/*Av*1 ratios below 2. Thus, in general, our results are consistent with those of Hageman & Burris (1978b). One important extra feature of our experiments is that the reduction of N_2 as well as protons is considered. If only NH_3 formation is considered, there is always an apparent decrease in *Av*2 specific activity at low ratios (high *Av*1) (e.g., Figure 6c). However, the *Av*2 specific activity for H_2 evolution continues to increase to the lowest ratios tested. We suggest, then, that this effect is more appropriately discussed as a change in allocation of electron flow rather than inhibition. When the data are normalized to the *Av*1 concentration (e.g., Figure 1c), the specific activity of *Av*1 increases steeply with the ratio (increasing *Av*2 concentration) up to ~10 and then more slowly but continuously to the highest ratios tested, as observed previously (Mortenson et al., 1976; Hageman & Burris, 1978b). This observation indicates that there are no higher complexes which are inactive and that there are probably rather low-affinity complexes, or simple bimolecular reactions, involved between *Av*2 and either *Av*1 or *Av*1–*Av*2 complexes in some steps of the reaction.

Electron Partitioning. Under D_2 but in the absence of N_2 (experiments 2 and 3), there is no change in allocation of electrons between H_2 and HD as a function of ratio (e.g., Figure 3b). The rate laws for H_2 and HD formation must then have the same dependence on *Av*2 concentration, such that the ratio of H_2 and HD formation rates is independent of the *Av*2 concentration. This result would be expected if H_2 and HD are produced from the same state of the enzyme. In addition, the yield of HD less than doubles on doubling the D_2 partial pressure, which may indicate partial saturation of a D_2-binding site or some more complex dependence of HD formation on D_2 pressure.

Under a N_2 atmosphere (experiments 4 and 5), the distribution of electron flow to NH_3 and H_2 varies as a function of the *Av*2/*Av*1 ratio (e.g., Figure 4b). For *Av*2/*Av*1 ratios up to 3, the percentage of electrons going to NH_3 rises from 0% to 30% under 40% N_2 and from 0% to 60% under 100% N_2. Above the *Av*2/*Av*1 ratio of 3, no further change in electron allocation occurs under 100% N_2, while under 40% N_2, the percentage giving NH_3 increases to 60% at ratios of 70–140. Thus, under our conditions, an upper limit of 60% of the electron flow goes to NH_3, as reported previously (Hadfield & Bulen, 1969; Rivera-Ortiz & Burris, 1975). This limit can be reached either by increasing the partial pressure of N_2 to 1 atm at a ratio of 3 (or lower) or by increasing the *Av*2/*Av*1 ratio at lower N_2 partial pressures. This behavior would be predicted from a mechanism in which an enzyme form which can produce H_2 can also reversibly bind N_2. This N_2–enzyme complex would form ammonia (2 mol), if enough free *Av*2 is available to continue the reduction, and the NH_3 produced would increase with N_2 partial pressure because more of this complex would be formed. Moreover, the NH_3 formed would also increase with *Av*2 concentration because increased reduction would be favored over N_2 dissociation to reform an enzyme state which could evolve H_2. This pattern of offsetting low N_2 pressures by high *Av*2/*Av*1 ratios is illustrated by the high yields of NH_3 under 100% N_2 and 40% N_2. At *Av*2/*Av*1 ratios of 0.5–20, about twice as much NH_3 is formed under the higher pressure, but at ratios above 50, the yield is about the same for both N_2 pressures. This observation indicates that the apparent K_m for N_2 decreases with increasing *Av*2/*Av*1 ratio.

Under an atmosphere of 50% D_2/40% N_2/10% Ar (experiment 6), the percentage of electron flow going to H_2 evolution decreases as the *Av*2/*Av*1 ratio increases, while that to both HD and NH_3 formation increases. Unlike the case in the absence of N_2, the fraction of electron flow to HD varies with the *Av*2/*Av*1 ratio, which suggests that HD is formed by two separate pathways, one N_2 independent and the other N_2 dependent (Burgess et al., 1981). The data under 50% D_2/50% Ar (see Figure 3b), which show that 6% of the electron flow normally giving H_2 is redirected to form HD, and the data from the N_2-dependence experiment in the following paper (Burgess et al., 1981) allow N_2-*dependent* HD formation to be calculated for the 50% D_2/40% N_2/10% Ar experiment as ($HD_{total} - 0.12H_2$). After such an adjustment, electron allocation to N_2-*dependent* HD formation, just like that to total HD formation, increases more rapidly than the allocation to NH_3 formation as the *Av*2/*Av*1 ratio is increased (Figure 6d).

The following paper details the relationships among N_2-*dependent* HD formation, N_2-*independent* HD formation, NH_3 formation, and H_2 evolution (Burgess et al., 1981) and shows

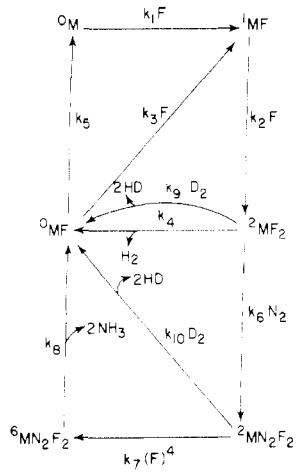

FIGURE 10: Proposed mechanism for substrate reduction by nitrogenase. M equals *Av*1, F equals *Av*2, superscripts equal the number of electrons associated with the complex, and subscripts equal the number of molecules of *Av*2 (F) or atoms of N associated with the complex. Units for the rate constants (k) are defined in Table I. Products are formed from the following steps: k_4 (ATP-dependent H_2 evolution); k_9 (N_2-independent HD formation); k_{10} (N_2-dependent HD formation); and k_8 (ammonia formation).

that, at an *Av*2/*Av*1 ratio of 5 and under 50% D_2, the ratio of N_2-*dependent* HD formation to NH_3 formation is *invariant* over a wide range of N_2 partial pressures. Under both 100% D_2 and 50% D_2/50% Ar, we find the ratio of N_2-*independent* HD to H_2 *invariant* over the wide range of component ratios. Figure 6d clearly shows, however, that the ratio of N_2-*dependent* HD formed to NH_3 produced does vary with the *Av*2/*Av*1 ratio, with lower ratios favoring N_2-*dependent* HD formation over NH_3 production. This observation is part of the general pattern of lower *Av*2/*Av*1 ratios favoring the formation of products that require fewer reducing equivalents. In addition, Figure 6b shows that the total electron flow going to NH_3 plus HD (which is mainly N_2 *dependent*) is 60% at the highest ratio, the same maximum as for NH_3 under 60% Ar/40% N_2 and 100% N_2.

Hydrazine reduction (experiment 7) shows a slight decrease in its percentage of total electron flow at high *Av*2/*Av*1 ratios. This pattern is different from that for all other substrates, including N_2 reduction. Further studies are contemplated to determine whether this pattern is typical of other substrates reduced by two electrons, such as acetylene.

Proposed Mechanism. The preceding observations, plus our N_2-dependence data (Burgess et al., 1981), form a basis for proposing mechanisms for nitrogenase action using the procedure presented under Materials and Methods. The mechanism which best depicts these data is shown in Figure 10. The reduction of *Av*2 and all steps involving MgATP are not explicitly shown because the levels of dithionite and MgATP were maintained at a constant, high level. All steps are represented as irreversible not only to minimize the number of parameters but also because electron transfer from *Av*2 appears coupled to MgATP hydrolysis. N_2 binding was made reversible in one trial, but the fit did not significantly improve. Since *Av*1 may contain either one dinuclear or two independent mononuclear active sites, both M equals *Av*1 concentration and M equals twice the *Av*1 concentration were tried in mechanistic fits, but no appreciable difference was observed. Here, we use M equals *Av*1.

The mechanism (Figure 10) is almost as simple as could be proposed. Hydrogen evolution (k_4) competes with N_2 binding (k_6) for one intermediate. Hydrogen evolution, as opposed to HD formation, is not allowed elsewhere, although

Table I: Rate Constants from the Mechanism for N_2 Reduction, H_2 Evolution, and HD Production (Figure 10)

rate constant	value	units
1	4.54 (10^4)	M^{-1} min^{-1}
2	3.38 (10^7)	M^{-1} min^{-1}
3	4.84 (10^4)	M^{-1} min^{-1}
4	1.50 (10^{-1})	min^{-1}
5	3.56 (10^{-1})	min^{-1}
6	7.20	atm^{-1} min^{-1}
7	1.04 (10^{25})	M^{-4} min^{-1}
8	1.34	min^{-1}
9	2.23	atm^{-1} min^{-1}
10	1.82 (10^4)	atm^{-1} min^{-1}

the reducing power is clearly available. The inclusion of the intermediate ^0MF (a complex with one *Av*2 bound per *Av*1, but with no reducing equivalents remaining) quite significantly improves the fit at ratios below 5. This complex can either decompose to liberate its components (k_5) or be reduced by free, reduced *Av*2 [k_3(F)]. Possible displacement of bound *Av*2 in the last process cannot be treated. The inclusion of ^0MF mandates the presence of ^1MF and, thus, the separation of the k_1 and k_2 steps. Binding of N_2 is separated from further reduction so that both N_2-dependent and N_2-independent HD are formed from a two-electron reduced state as required by the reaction stoichiometry. Reduction of $^2MN_2F_2$ is represented as a single step for simplicity of fitting (although it undoubtedly would occur in several steps) with a rate constant greater than predicted by four consecutive k_1 steps but smaller than for four consecutive k_2 steps. Ammonia release is shown as a separate step because the presence of $^6MN_2F_2$ significantly improves the fit.

The parameters for the best fit are listed in Table I. The best overall fit for 219 different assay conditions (means plus standard deviations for 608 observations) gives reduced χ^2 values for the individual data sets, *when treated simultaneously* with this mechanism, of (1) 3.6 for 100% Ar, (2) 7.9 for 100% D_2, (3) 2.9 for 50% D_2/50% Ar, (4) 5.9 for 100% N_2, (5) 6.2 for 40% N_2/60% Ar, and (6) 12.9 for 50% D_2/40% N_2/10% Ar. In general, the fit is better when individual data sets are treated alone, e.g., the 100% Ar data above give a reduced χ^2 = 1.22 and the 50% D_2/40% N_2/10% Ar data give a reduced χ^2 = 3.82. The fit is also better for the simpler experiments without N_2 reduction. Because a D_2-binding site is not part of the mechanism, the doubling of HD formation predicted when the D_2 pressure is doubled is not observed. However, for simplicity, a D_2-binding step is not included in our mechanism.

Figure 11 illustrates the strong points and problems with this mechanism. For this fit, all 609 observations are used, and the fit for the 100% N_2 experiment is selected as representative. Figure 11a–c shows that the general shape and magnitude of the activity vs. *Av*2/*Av*1 ratio plots are predicted by our mechanism for H_2, NH_3, and total electron flow. This general agreement is true for all experiments for H_2, HD, NH_3, and total electron flow. This mechanism does not require that total electron flow be independent of substrate and the fits are in close agreement with our observations which show a slight decrease in total electron flow with N_2 present. Figure 11d shows the fit normalized to *Av*1, which is quite consistent with the observed rapid increase in activity below a ratio of ~10, followed by a continuing slower increase. The overall fit of this mechanism is not totally satisfactory because it fails to predict significant events that occur at low ratios. Figure 11e shows that this mechanism fails to predict the decrease in *Av*2 activity observed at very low *Av*2/*Av*1 ratios for NH_3 for-

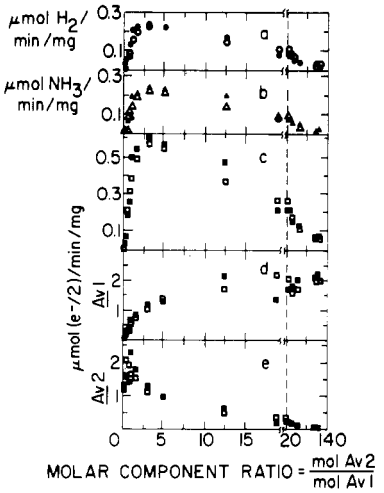

FIGURE 11: Calculated and observed values for the 100% N_2 experiment (number 4). Open symbols represent calculated values, and closed symbols represent observed values. If calculated equals observed, only the observed value is shown. Calculated values were obtained by simultaneously fitting the data obtained for experiments 1–6 plus the N_2-dependence data from the following paper to the mechanism in Figure 10 (see Materials and Methods). Plots of (a) micromoles of H_2 evolved per min per milligram of total protein vs. ratio, (b) micromoles of NH_3 formed per minute per milligram of total protein vs. ratio, (c) micromoles of total electron pairs to both products per minute per milligram of total protein vs. ratio, (d) micromoles of total electron pairs per minute per milligram of *Av*1 vs. ratio, and (e) micromoles of total electron pairs per minute per milligram of *Av*2 vs. ratio. Details are given in the legends of Figures 1 and 3.

mation and, consequently, the leveling off of *Av*2 specific activity for total electron flow at *Av*2/*Av*1 ratios below 2. Another, possibly related, problem occurs with electron allocation to the different products as a function of *Av*2/*Av*1 ratio. Under 100% N_2, Figure 4b clearly shows that low ratios favor H_2 evolution over NH_3 formation, a trend not predicted by our mechanism, which instead gives 60% of the electron flow to NH_3 and 40% to H_2 at all *Av*2/*Av*1 ratios. Future experiments will concentrate on these significant changes at low ratios.

Our approach is a valid one for setting limiting conditions on the mechanistic possibilities for nitrogenase turnover. Accurate fits should eventually become independently testable when individual states, like those in Figure 10, become identified with spectroscopic parameters observed under steady-state conditions by EPR, Mössbauer, or X-ray absorption spectroscopy. We believe that this correspondence is not yet firmly established, so that attempts to apply this procedure are premature. We plan, therefore, to continue to pursue fitting schemes, such that the product formation curves and steady-state intermediate levels can be predicted and compared with other experiments. Despite the lack of complete fits at present, the available data have indicated the optimal conditions for the measurement and subsequent interpretation of the HD formation, H_2 inhibition, and H_2 evolution reactions of nitrogenase. The resulting data and their detailed interpretation in terms of molecular mechanisms are the subjects of the following paper (Burgess et al., 1981).

Acknowledgments

We thank Dr. J. L. Corbin for providing creatine phosphate.

Supplementary Material Available

Seven tables showing the results for all experiments (7 pages). Ordering information is given on any current masthead page.

References

Anatol, S. (1961) French Patent 1 211 099.

Bergerson, F. J., & Turner, G. L. (1973) *Biochem. J. 131*, 61–75.

Bevington, P. R. (1969) *Data Reduction and Error Analysis for the Physical Sciences*, p 336, McGraw Hill, New York.

Bulen, W. A. (1976) *Proc. Int. Symp. Nitrogen Fixation, 1st, 1974 1*, 177–186.

Bulen, W. A., & LeComte, J. R. (1966) *Proc. Natl. Acad. Sci. U.S.A. 56*, 979–986.

Bulen, W. A., Burns, R. C., & LeComte, J. R. (1965) *Proc. Natl. Acad. Sci. U.S.A. 53*, 532–539.

Burgess, B. K., Jacobs, D. B., & Stiefel, E. I. (1980) *Biochim. Biophys. Acta 614*, 196–209.

Burgess, B, K., Wherland, S., Newton, W. E., & Stiefel, E. I. (1981) *Biochemistry* (following paper in this issue).

Burris, R. H. (1972) *Methods Enzymol. 24B*, 415–431.

Chaykin, S. (1969) *Anal. Biochem. 31*, 375–382.

Corbin, J. L. (1978) *Anal. Biochem. 84*, 340–342.

Davis, L. C., Shah, V. K., & Brill, W. J. (1975) *Biochim. Biophys. Acta 403*, 67–77.

Eady, R. R. (1973) *Biochem. J. 135*, 531–535.

Eady, R. R., Smith, B. E., Cook, K. A., & Postgate, J. R. (1972) *Biochem. J. 128*, 655–675.

Emerich, D. W., & Burris, R. H. (1976a) *J. Bacteriol. 134*, 936–943.

Emerich, D. W., & Burris, R. H. (1976b) *Proc. Natl. Acad. Sci. U.S.A. 73*, 4369–4373.

Haaker, H., & Veeger, C. (1977) *Eur. J. Biochem. 77*, 1–10.

Hadfield, K. L., & Bulen, W. A. (1969) *Biochemistry 8*, 5103–5108.

Hageman, R. V., & Burris, R. H. (1978a) *Biochemistry 17*, 4117–4124.

Hageman, R. V., & Burris, R. H. (1978b) *Proc. Natl. Acad. Sci. U.S.A. 75*, 2699–2702.

Hageman, R. V., & Burris, R. H. (1979) *J. Biol. Chem. 254*, 11189–11192.

Hageman, R. V., & Burris, R. H. (1980) in *Molybdenum and Molybdenum-Containing Enzymes* (Coughlan, M. P., Ed.) pp 403–426, Pergamon Press, New York.

Hoch, G. E., Schneider, K. C., & Burris, R. H. (1960) *Biochim. Biophys. Acta 37*, 273–279.

Hwang, J. L., Chen, C. H., & Burris, R. H. (1973) *Biochim. Biophys. Acta 292*, 256–270.

King, E. L., & Altman, D. (1956) *J. Phys. Chem. 60*, 1375–1378.

Ljones, T., & Burris, R. H. (1972) *Biochim. Biophys. Acta 321*, 103–113.

Ljones, T., & Burris, R. H. (1978) *Biochem. Biophys. Res. Commun. 80*, 22–25.

Mortenson, L. E., & Thorneley, R. N. F. (1979) *Annu. Rev. Biochem. 48*, 387–418.

Mortenson, L. E., Walker, M. N., & Walker, G. A. (1976) *Proc. Int. Symp. Nitrogen Fixation, 1st, 1974 1*, 117–149.

Newton, W. E., Bulen, W. A., Hadfield, K. L., Stiefel, E. I., & Watt, G. D. (1977) *Recent Dev. Nitrogen Fixation*, [*Proc. Int. Symp.*], *2nd, 1976*, 119–130.

Orme-Johnson, W. H., Davis, L. C., Henzl, M. T., Averill, B. A., Orme-Johnson, N. R., Munck, E., & Zimmerman, R. (1977) *Recent Dev. Nitrogen Fixation*, [*Proc. Int. Symp.*], *2nd, 1976*, 131–178.

Rivera-Ortiz, J. M., & Burris, R. H. (1975) *J. Bacteriol. 123*, 537–545.

Shah, V. K., Davis, L. C., & Brill, W. J. (1972) *Biochim. Biophys. Acta 256*, 498-511.
Shah, V. K., Davis, L. C., Gordon, J. K., Orme-Johnson, W. H., & Brill, W. J. (1973) *Biochim. Biophys. Acta 292*, 246-270.
Silverstein, R., & Bulen, W. A. (1970) *Biochemistry 9*, 3809-3815.
Smith, B. E. (1977) *J. Less-Common Metals 54*, 465-475.
Thorneley, R. N. F., Eady, R. R., & Yates, M. G. (1975) *Biochim. Biophys. Acta 403*, 269-284.
Vandercasteele, J.-P., & Burris, R. H. (1970) *J. Bacteriol. 101*, 794-801.
Watt, G. D. (1980) in *Molybdenum Chemistry of Biological Significance* (Newton, W. E., & Otsuka, S., Eds.) pp 3-21, Plenum Press, New York.
Watt, G. D., & Burns, A. (1977) *Biochemistry 16*, 264-270.
Wilson, P. W., & Umbreit, W. W. (1937) *Arch. Mikrobiol. 8*, 440-457.
Winter, H. C., & Burris, R. J. (1976) *Annu. Rev. Biochem. 45*, 409-426.

Nitrogenase Reactivity: Insight into the Nitrogen-Fixing Process through Hydrogen-Inhibition and HD-Forming Reactions†

Barbara K. Burgess, Scot Wherland,‡ William E. Newton,* and Edward I. Stiefel

ABSTRACT: The dihydrogen reactions of nitrogenase are H_2 evolution, H_2 inhibition of N_2 reduction, and HD production from H_2/D_2O or D_2/H_2O. The relationships among these dihydrogen reactions are studied to gain insight into the mechanism of N_2 reduction. Detailed studies have probed (1) the formation of HD by nitrogenase as a function of partial pressures of N_2, D_2, and CO, (2) the formation of TOH from T_2 under N_2-fixing conditions, and (3) the reduction of hydrazine by nitrogenase. Experiments under T_2 demonstrate that negligible tritium is incorporated into water compared to the HD produced under similar conditions. Studies of total electron flow, in the presence or absence of D_2, establish a requirement of 1 mol of electrons/mol of HD formed. These findings show definitively that HD formation is *not* due to a simple H_2O/D_2 exchange mechanism. Kinetic analysis shows that HD is produced by two separate processes. In the minor process, the HD formed is proportional to the H_2 evolved, electron requiring, and partially inhibited by 1% CO. In the major process, HD formation is dependent on N_2 pressure, electron requiring, and completely inhibited by CO. A mechanism is proposed whereby HD from the N_2-dependent process is formed from a bound, reduced dinitrogen intermediate. This mechanism is supported by studies using hydrazine as a substrate for nitrogenase and leads to the conclusion that H_2 inhibition of nitrogen fixation and N_2-dependent HD formation are manifestations of the same molecular process.

The dihydrogen reactions of nitrogenase have been extensively studied in vitro (Jackson et al., 1968; Bulen, 1976; Stiefel et al., 1977; Newton et al., 1977) and in vivo [e.g., Evans et al. (1980)]. In the absence of other reducible substrates, all of the reductant consumed by nitrogenase is used to reduce protons to H_2 in the ATP[1]-dependent H_2 evolution reaction (Bulen et al., 1965). When N_2 is added as a reducible substrate, an extrapolated maximum of 75% of the electrons reduce N_2 while the remainder reduce protons (Hadfield & Bulen, 1969; Rivera-Ortiz & Burris, 1975). Dihydrogen is not only a product of nitrogenase turnover but is also an inhibitor of N_2 reduction (Wilson & Umbreit, 1937). H_2 (and, by implication, D_2) inhibition is specific for N_2 reduction and does not affect either the reduction of other nitrogenase substrates or its own evolution (Hwang et al., 1973). The apparent competitive nature of this inhibition was first demonstrated in red clover plants (Wilson & Umbreit, 1937) and later in other organisms including *Azotobacter vinelandii* (*Av*) (Strandberg & Wilson, 1967; Hadfield & Bulen, 1969; Hwang et al., 1973).

Hoch et al. (1960) showed that both H_2 evolution and HD formation occurred in soybean nodules under a D_2/N_2 atmosphere and that the latter was stimulated by N_2 and inhibited by either CO (an inhibitor of N_2 reduction) or N_2O (an alternative substrate). They suggested that HD formation occurred by a reversible exchange of D_2 with an enzyme-bound diazene intermediate (Hoch et al., 1960). However, later attempts to trap and so identify diazene as an intermediate in N_2 reduction were unsuccessful (Burris et al., 1965). Other workers confirmed these results with both the soybean nodule system (Bergerson, 1963; Turner & Bergerson, 1969) and cell-free preparations from the free-living, N_2-fixing microorganism *A. vinelandii* (Jackson et al., 1968). These studies also showed that HD formation required ATP and reductant and supported speculation that HD was formed by a reversible exchange of D_2 with an enzyme-bound diazene-, hydrazine-, and/or amine-level intermediate. Hwang et al. (1973) reported that the enhancement of HD formation by N_2 was more pronounced for *Av* nitrogenase than for the *Clostridium pasteurianum* system.

Recognizing the potential for obtaining information concerning the mechanism of N_2 reduction from quantitation of this phenomenon, Bulen (1976), using the purified *Av* nitrogenase complex (Hadfield & Bulen, 1969; Bulen & Le-

† Contribution No. 733 from the Charles F. Kettering Research Laboratory, Yellow Springs, Ohio 45387. *Received July 29, 1980; revised manuscript received April 2, 1981.* This study was supported in part by Project No. 79-00359 from SEA/CGO of the U.S. Department of Agriculture. S.W. was supported by a National Science Foundation National Needs Postdoctoral Fellowship.

‡ Present address: Department of Chemistry, Washington State University, Pullman, WA 99163.

[1] Abbreviations used: ATP, adenosine 5′-triphosphate; $NaDodSO_4$, sodium dodecyl sulfate, cpm, counts per minute; dppe, 1,2-bis(diphenylphosphino)ethane.

0006-2960/81/0420-5140$01.25/0